Desalination and Water Treatment
www.deswater.com
doi: 10.5004/dwt.2020.25155

195 (2020) 1–7
August

Theoretical and experimental investigation of multistage submerged vacuum membrane distillation

Yongjun Choi, Jaehyun Ju, Jihyeok Choi, Sangho Lee*

School of Civil and Environmental Engineering, Kookmin University, 77 Jeongneung-ro, Seoungbukgu, Seoul 02707, Republic of Korea, Tel. +82-2-910-4529; Fax: +82-62-910-4939; email: sangholee@kookmin.ac.kr (S. Lee)

Received 1 July 2019; Accepted 18 November 2019

ABSTRACT

A multistage submerged vacuum membrane distillation system (SVMD) offers a novel approach to increase thermal energy efficiency by recovering the latent heat in the vapor from the membrane. However, most studies have focused on single-stage direct contact membrane distillation systems with lower thermal efficiency. This study investigated the feasibility of a multistage SVMD system for seawater desalination to provide insight into the design of MD systems. A theoretical model to predict the performance of the multistage SVMD was developed. A bench-scale experimental device was fabricated to experimentally evaluate the efficiency of the multistage SVMD system and verify the theoretical model. A hollow fiber MD membrane made of polyvinylidene fluoride was used. The experimental results show that the three-stage SVMD can significantly reduce the thermal energy requirement with a slight trade-off of the overall flux. Moreover, the theoretical model is useful in predicting the performance of the multistage SVMD system at different operating conditions.

Keywords: Vacuum membrane distillation; Submerged; Multistage; Theoretical model

1. Introduction

Membrane distillation (MD) is a thermally driven separation process that allows water vapor transport through hydrophobic porous membranes [1,2]. MD systems can be classified into four basic configurations depending on the condensation methods: direct contact membrane distillation (DCMD), air-gap membrane distillation, sweeping gas membrane distillation, and vacuum membrane distillation (VMD) [3]. The driving force in an MD system is the vapor pressure difference across the membrane that is created by the temperature difference between the two sides of the membrane [1]. The MD is driven by vapor pressure; hence, it is not significantly affected by the osmotic pressure gradient across the membrane, and highly concentrated salt solutions close to the saturation point can be obtained [4]. The MD is a relatively new and promising technology for brackish and seawater desalination [5]. It is more resistant to fouling because of its low operating pressure [6], and it produces high-quality water because only the water vapor passes through the membrane pores [7]. However, the MD has several drawbacks, such as temperature polarization effects and high thermal energy consumption as well as heat loss [8]. Despite being under investigation for several decades, the MD process is still in its early stage in terms of commercial applications even at small-scale applications [9]. Therefore, further work is still required to bring MD technologies into practice, including the development of new MD membranes, modules, and module configurations and design of optimization systems aiming to maximize the water vapor flux, significant conductive losses, and low thermal efficiency.

The multistage submerged vacuum membrane distillation system (SVMD) offers a novel approach to increasing

* Corresponding author.

thermal energy efficiency by recovering the latent heat in the vapor from the membrane and eliminating the heat loss from feed recirculation and reheating. However, most studies have focused on single-stage DCMD systems that have a lower thermal efficiency [10,11].

The present study investigates the feasibility of a multistage SVMD system for seawater desalination to provide insight into the design of MD systems. A theoretical model for predicting the performance of the multistage SVMD is also developed. Moreover, a bench-scale experimental device is fabricated to experimentally evaluate the efficiency of the multistage SVMD system and verify the theoretical model.

2. Material and methods

2.1. MD model

The driving force in the VMD process is maintained by applying a continuous vacuum at the permeate side below the equilibrium vapor pressure. The hot feed solution is brought into contact with one side of a hydrophobic microporous membrane. The water vapor flux J_w in the case of the mass transport of water through the membrane is expressed as follows [6,12]:

$$J_w = A_B\left[P_v\left(T_m, C_m\right) - P_0\right] \tag{1}$$

where A_B is the VMD coefficient of the membrane, T_m is the temperature on the membrane surface in the feed side, C_m is the concentration on the membrane surface in the feed side, $P_v(T_m, C_m)$ is the water vapor pressure on the membrane surface in the feed side, and P_0 is the pressure in the vacuum side.

The water vapor pressure on the membrane surface in the feed side may be related with the temperature and feed solution concentration. The vapor pressure, $P_v(T_m, C_m)$ is expressed as follows [13]:

$$P_v\left(T_m, C_m\right) = \frac{\exp\left(aT_m^{-1} + bT_m + cT_m^2 + dT_m^3 + e\log\left(T_m\right)\right)}{1 + 0.57257\left(\frac{C_m}{1000 - C_m}\right)}$$
$$a = -5.80 \times 10^3$$
$$b = 1.39 - 4.86 \times 10^{-2}$$
$$c = 4.18 \times 10^{-3} \tag{2}$$
$$d = -1.48 \times 10^{-8}$$
$$e = 6.55$$

where C_m is calculated according to film theory to interpret the concentration polarization, while the solvent concentration profile on the surface can be calculated according to the following equation [14]:

$$\frac{C_m}{C_b} = \exp\left(\frac{J_w}{k}\right) \tag{3}$$

where C_b is the concentration in the feed bulk solution, and k is the mass transfer coefficient for the back diffusion of the solute from the membrane to the bulk solution. The mass transfer coefficient k can be calculated similar to the RO.

In a general MD process, the mass transfer may be explained in principle based on different possibilities: Knudsen flow model, viscous flow model, molecular diffusion model, or a combination of them [6,15]. In a VMD configuration, the molecular diffusion model may not be an adequate representation of the mass transfer in view of the low partial pressure of air inside the pores. Thus, the mass transport mechanisms through the hydrophobic micro-porous membrane in the VMD could either be a Knudsen flow model, a viscous flow model, or a combination of both [6,15]. The average pore diameter of the MD membrane is commonly smaller than the mean free path of the water vapor. Hence, the Knudsen flow model is adopted by majority of the mass transport mechanisms in the VMD configuration [15]. In the Knudsen flow model, A_B is expressed as follows [15]:

$$A_B = \frac{MD^{\mathrm{kn}}}{RT_m\delta} \tag{4}$$

$$D^{\mathrm{kn}} = \frac{2\varepsilon r}{3\tau}\left(\frac{8RT_m}{\pi M}\right)^{0.5} \tag{5}$$

where M is the water molecular mass, D_{kn} is the Knudsen diffusion coefficient, R is the gas constant, δ is the membrane thickness, ε is the porosity, r is the pore size, and τ is the pore tortuosity. MD involves the mass transfer of the water vapor coupled with heat transfer across the membrane. The heat transfer across the membrane boundary layer in an MD system is a limiting step for mass transfer because a large quantity of heat must be applied to the vapor–liquid interface to vaporize the liquid. In an MD system, heat transfer occurs through latent heat transfer that accompanies the vapor flux and conduction heat transfer across the membrane [1]. Consequently, a rather complex relationship exists between heat and mass transfer. This problem is related and involved with the presence of an unstirred boundary layer that adjoins the membrane, implying that the temperature at the membrane surface, T_m is lower than the corresponding value at the well-stirred bulk phase, T_b. This phenomenon is called temperature polarization, and masks the real magnitude of the driving force [1]. However, in a VMD configuration, the conductive heat across the membrane is negligible because of the low pressure on the permeate side of the membrane [1]. Hence, the heat flux through the liquid boundary layer can be represented using the following equation [15]:

$$h_w\left(T_m - T_b\right) = J_w\Delta H_v \tag{6}$$

where ΔH_v is the latent heat of vaporization, h_w is the heat transfer coefficient, T_b is the feed bulk temperature, and T_m is the temperature in the membrane surface. The heat transfer coefficient is calculated in a similar manner to the mass transfer coefficient [6,15].

$$h_w = \frac{K_m\mathrm{Nu}}{dh} \tag{7}$$

$$\mathrm{Nu} = 1.86\left(\mathrm{Re}\cdot\mathrm{Pr}\cdot\frac{dh}{L}\right)^{0.33} \quad \left(\mathrm{Re} \le 2{,}100\right) \tag{8}$$

$$\mathrm{Nu} = 0.023\,\mathrm{Re}^{0.8}\,\mathrm{Pr}^{0.33} \quad \left(\mathrm{Re} > 2{,}100\right) \tag{9}$$

2.2. MD membrane

Table 1 shows the MD membrane properties. A hollow fiber (Econity, Korea) membrane was used in this study. The mean pore size of the membranes was 0.1 μm, and the porosity was 70%. The membrane was made of polyvinylidene fluoride. The inner and outer diameters of the membrane were 0.8 and 1.2 mm, respectively.

2.3. MD experimental device

Figs. 1 and 2 show the single and two-stage SVMD setups used herein. The hollow fiber membrane with a total effective membrane area of approximately 78 cm^2 was used in the module. The system comprised a feed tank, a permeate tank, a submerged MD module, a heater, a cooler, a vacuum pump, and a heat exchanger. The system temperature and pressure were measured in real-time using temperature probes in the feed tank and permeate line and a pressure transducer in the permeate line. The permeate flux was calculated based on the weight difference measured by an electronic balance. The feed tank temperature ranged from 60°C to 80°C, while the permeate vapor

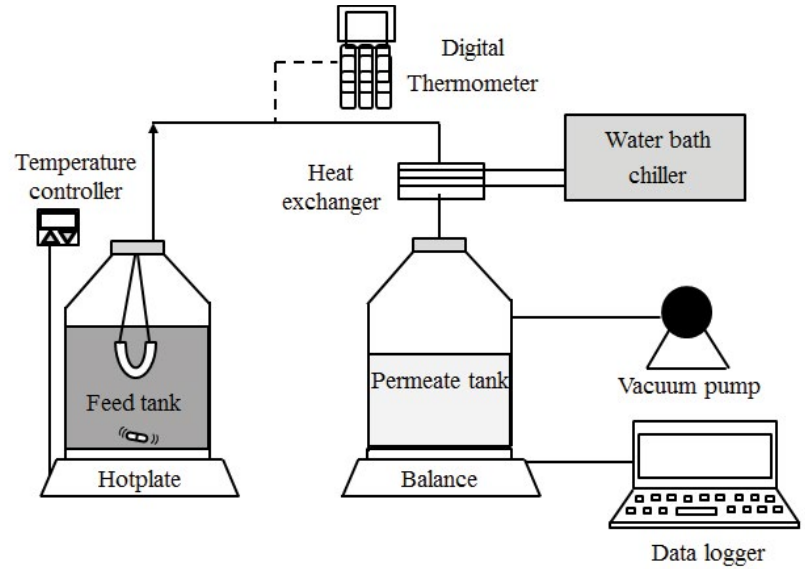

Fig. 1. Single-stage SVMD experimental device.

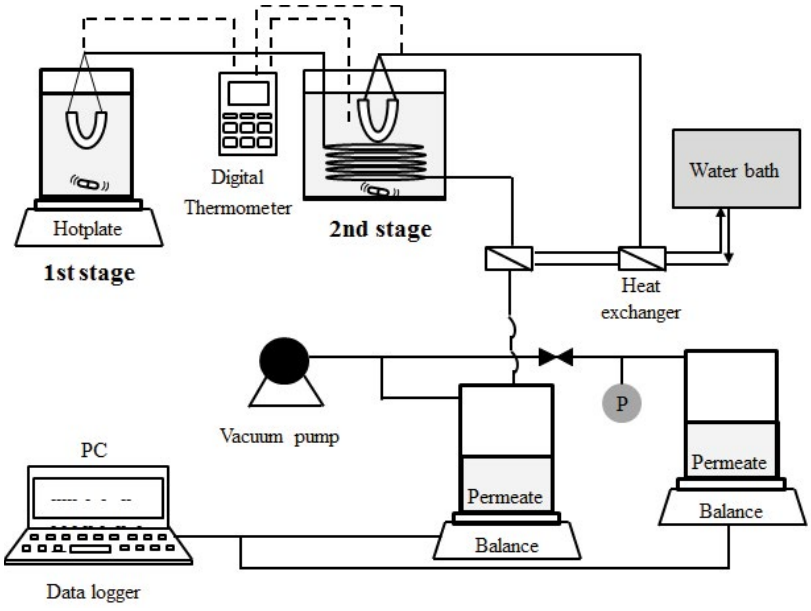

Fig. 2. Two-stage SVMD experimental device.

Table 1
MD membrane properties

Material	Polyvinylidene fluoride
Pore size (μm)	0.1
Inside diameter (μm)	0.07
Outside diameter (μm)	0.12
Porosity	0.7
Tortuosity	2.0
Length (cm)	0.15

temperature ranged from 0.1 to 0.45 bar(a). The feed water was a 35,000 mg/L NaCl solution. Table 2 summarizes the MD experiment conditions.

3. Results and discussions

First, the performance of the single-stage SVMD system was evaluated to find the optimum experimental conditions of a three-stage SVMD system using 35,000 mg/L NaCl solution as the feed water. The feed solution was directed to the outside of the hollow fiber membrane. The vacuum pressure was applied into the side of the hollow fiber membrane. The filtration time for each experiment was 3 h.

Figs. 3 and 4 show the variation in the permeate flux and permeate vapor temperature, respectively, according to the feed temperature and vacuum pressure in a single-stage SVMD operation.

The permeate flux and the permeate vapor temperature were significantly affected by the feed temperature and the vacuum pressure. The permeate flux ranged from 1.6 to 39.9 LMH. Meanwhile, the permeate vapor temperature ranged from 45.5°C to 78.3°C. The driving force of the VMD was the vapor pressure difference; hence, the flux increased with an increase in the feed temperature and a decrease in the vacuum pressure. The permeate vapor temperature increased with an increase in the vacuum pressure. The permeate vapor temperature at the same vacuum pressure was nearly the same, regardless of the feed temperature.

A theoretical model for predicting the performance of the multistage SVMD was applied to the experimental data. Figs. 5 and 6 present the model fits of the MD model. The model results matched the experimental data very well [R^2 value = 0.96 (permeate flux), 0.94 (permeate vapor temperature)], indicating that the theoretical MD model has the potential to predict the permeate flux and the permeate vapor temperature in the SVMD system. According to the model fit results, the permeate vapor temperature was determined by only the vacuum pressure in the SVMD system. In other words, the permeate vapor temperature was equal to the saturated vapor pressure.

Three operating conditions were selected after evaluating the performance of the single-stage SVMD to find the design conditions of the three-stage SVMD system with a temperature drop of 10°C between each stage. Table 3 shows the results of the design value of the three-stage SVMD system. The feed temperature at each stage was 80°C, 70°C, and 60°C. The vacuum pressure at each stage was 0.4, 0.25, and 0.15 bar(a) to maintain the temperature difference of 5°C between the feed and permeate vapor in each stage. The thermal energies of the first and second stages were set to one and a half times to obtain the stable flux and temperature by extending the applied membrane area. The membrane area was set as 170, 141, and 141 cm^2 at each stage.

The performance of the three-stage SVMD was evaluated in two steps using a two-stage SVMD experimental device. First, the first- and second-stage experimental conditions were evaluated using the two-stage SVMD experimental device. After which, the second- and third-stage experimental conditions were tested using the two-stage SVMD experimental device. In the two-stage SVMD experiments, the feed temperature of the following stage was heated by the vapor from the previous-stage membrane.

Table 2
Summary of the experimental conditions for the single-stage submerged MD test

Feed temperature (°C)	Vacuum pressure (bar(a))
60	0.1, 0.15
65	0.1, 0.15, 0.2
70	0.1, 0.15, 0.2, 0.25
75	0.1, 0.15, 0.2, 0.25, 0.3, 0.35
80	0.1, 0.15, 0.2, 0.25, 0.3, 0.35, 0.44, 0.45

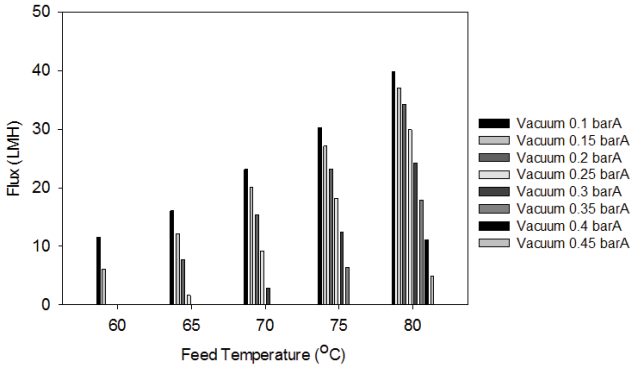

Fig. 3. Permeate flux according to the feed temperature and vacuum pressure in a single-stage SVMD.

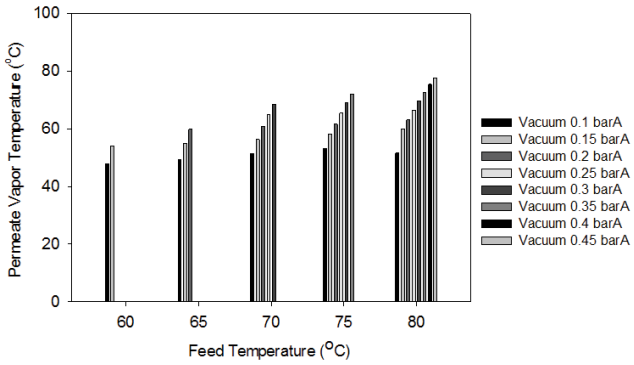

Fig. 4. Permeate vapor temperature according to the feed temperature and vacuum pressure in a single-stage SVMD.

Fig. 7 shows the permeate flux variations in the first- and second-stage experimental conditions. The experiment was conducted for 5 h. The permeate flux remained steady during the filtration period. The average permeate flux during the filtration period was 11.0 and 9.0 LMH under the first- and second-stage experimental conditions, respectively.

Fig. 8 illustrates the variations of the feed and permeate vapor temperature in the first- and second-stage experimental conditions.

The feed and permeate vapor temperature remained steady during the filtration period like the permeate flux during the filtration period. The permeate vapor temperatures during the filtration period were 75.1°C and 63.9°C under the first- and second-stage experimental conditions, respectively.

The permeate flux and the permeate vapor temperature of each stage in the two-stage SVMD system were the same as those in the single-stage SVMD system.

Fig. 9 depicts the variations of the permeate flux in the second- and third-stage experimental conditions. The experiment was conducted for 5 h similar to the previous test. The permeate flux remained steady during the filtration period. The average permeate flux during the filtration period was 9.2 and 6.2 LMH under the second- and third-stage experimental conditions, respectively.

Fig. 10 shows the variations of the feed and permeate vapor temperature in the second- and third-stage experimental conditions. The feed and permeate vapor temperature remained steady during the filtration period like the permeate flux. The permeate vapor temperature during the filtration period was 64.2°C and 53.5°C under the first- and second-stage experimental conditions, respectively.

The permeate flux and the permeate vapor temperature of each stage for the second- and third-stage experimental conditions were similar to those for the single-stage SVMD system.

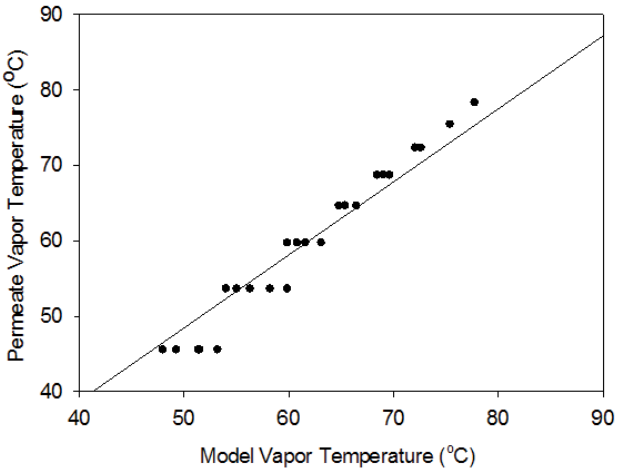

Fig. 6. Comparison between the saturated temperature and the permeate vapor temperature (R^2 = 0.94).

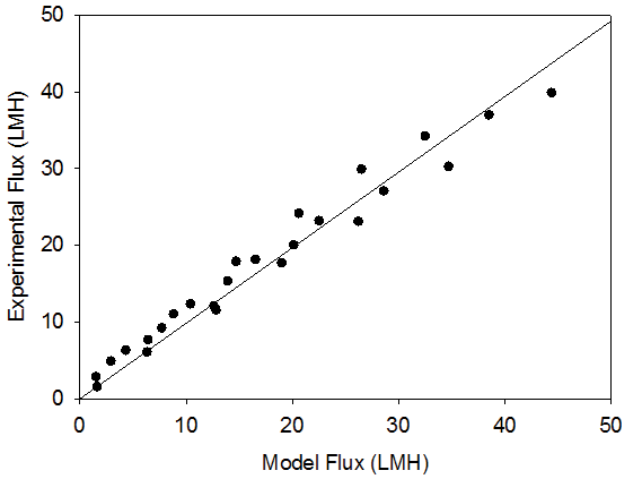

Fig. 5. Comparison between the model flux and the experimental flux (R^2 = 0.96).

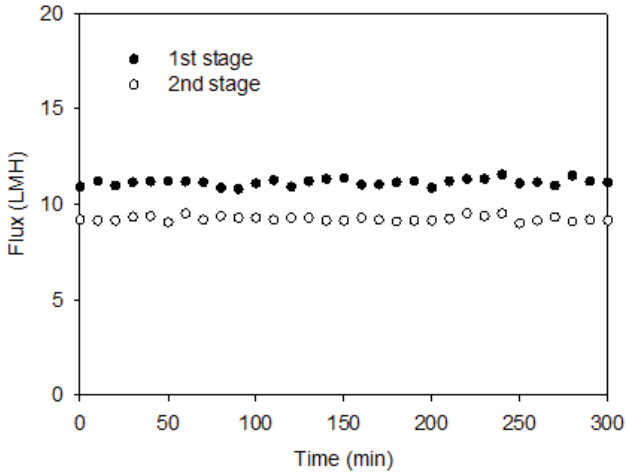

Fig. 7. Permeate flux variation according to the feed temperature and vacuum pressure in first- and second-stage experimental conditions

Table 3
Design conditions of the three-stage SVMD system with a temperature drop of 10°C between each stage

Stage	Feed temperature (°C)	Permeate vapor temperature (°C)	Flux (LMH)	Vacuum pressure (bar(a))	Calculated thermal energy (W)	Applied thermal energy (W)
1st	80	75.4	11.1	0.40	53.9	119.4
2nd	70	64.8	9.2	0.25	53.9	81.3
3rd	60	54.1	6.1	0.15	53.9	53.9

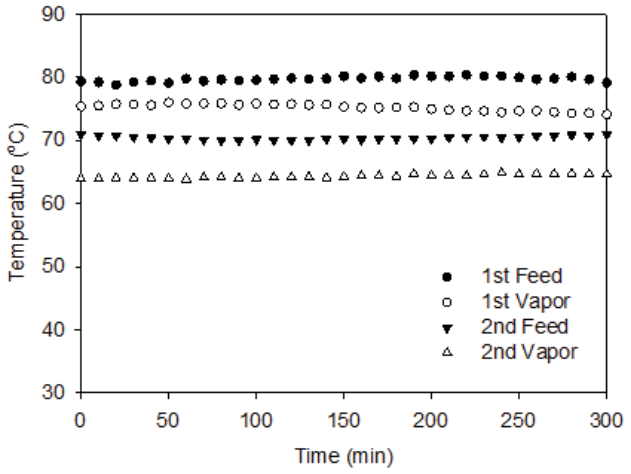

Fig. 8. Feed and permeate vapor temperature variation according to the feed temperature and vacuum pressure in the first- and second-stage experimental conditions.

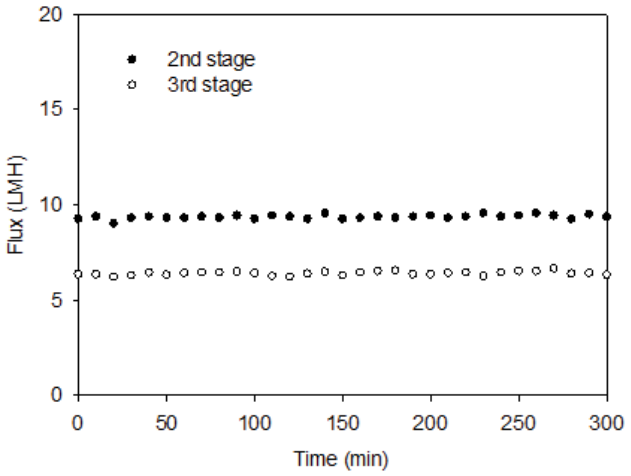

Fig. 9. Permeate flux variation according to the feed temperature and the vacuum pressure in the second- and third-stage experimental conditions.

Fig. 11 presents the thermal efficiency of the SVMD according to the number of stages. The thermal efficiency is defined as the ratio of the heat transfer rate for water evaporation over the total heat transfer rate. The thermal efficiency is very high in the SVMD. The ideal thermal efficiency is the same as the number of stages in the SVMD system, but the actual thermal efficiency is decreased because of the heat loss from the feed tank, pipe, and heat exchange. The thermal efficiency was 0.9, 1.5, and 1.9 according to the number of stages and heat loss and membrane area.

4. Conclusions

This study experimentally and theoretically investigated the effect of the initial heating temperature and vacuum pressure on the flux and thermal efficiency of the

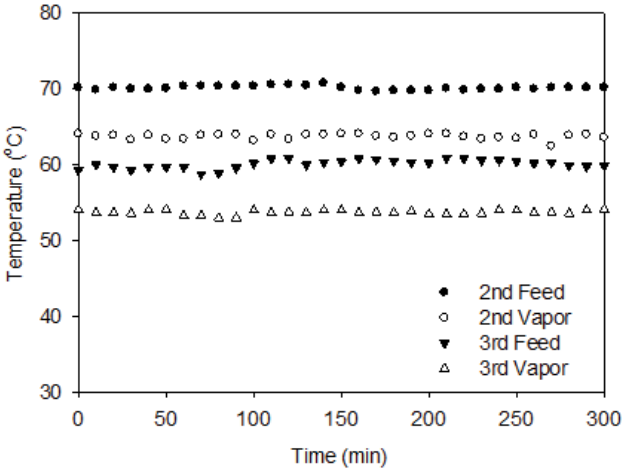

Fig. 10. Feed and permeate vapor temperature variation according to the feed temperature and the vacuum pressure in the second- and third-stage experimental conditions.

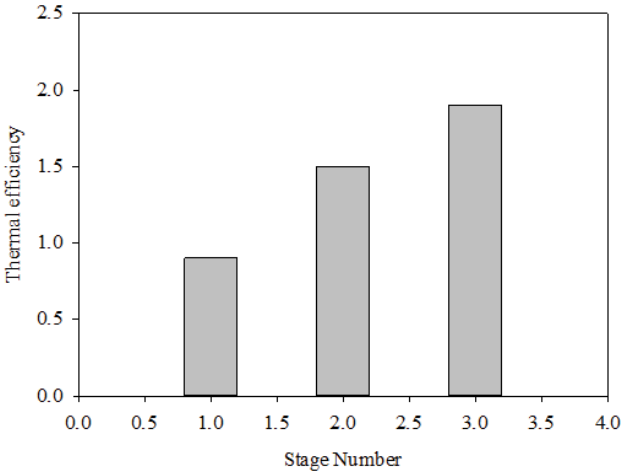

Fig. 11. Thermal efficiency of the SVMD according to the stage number.

single and multistage SVMD. Significant conclusions can be drawn from this work. The model results matched the experimental data very well, indicating that a theoretical model is useful in predicting the performance of the multistage SVMD system at different operating conditions. The three-stage vacuum VMD system shows a reasonable operating performance with an average flux at approximately 9.0 LMH using the model seawater (TDS 35,000 mg/L) as the feed water. Multistage submerged MD systems can have significantly higher thermal efficiencies than their single-stage system counterparts. Accordingly, the thermal efficiency in the SVMD system should be improved by increasing the number of stages.

Acknowledgment

This study was supported by Korea Ministry of Environment as "Global Top Project" (2017002100001).

References

[1] K.W. Lawson, D.R. Lloyd, Review: membrane distillation, J. Membr. Sci., 124 (1997) 1–25.

[2] M.S. El-Bourawi, Z. Ding, R. Ma, M. Khayet, A framework for better understanding membrane distillation separation process, J. Membr. Sci., 285 (2006) 4–29.

[3] E. Drioli, A. Ali, F. Macedonio, Membrane distillation: recent developments and perspectives, Desalination, 356 (2015) 56–84.

[4] M. Gryta, The concentration of geothermal brines with iodine content by membrane distillation, Desalination, 325 (2013) 16–24.

[5] D.L. Shaffer, L.H. Arias-Chavez, M. Ben-Sasson, S. Romero-Vargas Castrillón, N.Y. Yip, M. Elimelech, Desalination and reuse of high-salinity shale gas produced water: drivers, technologies, and future directions, Environ. Sci. Technol., 47 (2013) 9569–9583.

[6] M. Khayet, T. Matsuura, Membrane Distillation: Principles and Applications, Elsevier, Amsterdam, 2011.

[7] D.M. Warsinger, J.S. Waminathan, E. Guillen-Burrieza, H.A. Arafat, J.H. Lienhard V, Scaling and fouling in membrane distillation for desalination applications: a review, Desalination, 356 (2015) 294–313.

[8] J.-P. Mericq, S. Laborie, C. Cabassud, Evaluation of systems coupling vacuum membrane distillation and solar energy for seawater desalination, Chem. Eng. J., 166 (2011) 596–606.

[9] N. Thomas, M.O. Mavukkandy, S. Loutatidou, H.A. Arafat, Membrane distillation research & implementation: lessons from the past five decades, Sep. Purif. Technol., 189 (2017) 108–127.

[10] G. Chen, Y. Lu, W.B. Krantz, R. Wang, A.G. Fane, Optimization of operating conditions for a continuous membrane distillation crystallization process with zero salty water discharge, J. Membr. Sci., 450 (2014) 1–11.

[11] F. Edwie, T.-S. Chung, Development of simultaneous membrane distillation-crystallization (SMDC) technology for treatment of saturated brine, Chem. Eng. Sci., 98 (2013) 160–172.

[12] R.W.A. Schofield, A.G. Fane, C.J.D. Fell, Heat and mass transfer in membrane distillation, J. Membr. Sci., 33 (1987) 299–313.

[13] H.M. Sharqawy, H.L.V. John, M.Z. Syed, Thermophysical properties of seawater: a review of existing correlations and data, Desal. Water Treat., 16 (2010) 354–380.

[14] S. Lee, R.M. Lueptow, Membrane rejection of nitrogen compounds, Environ. Sci. Technol., 35 (2001) 3008–3018.

[15] J.I. Mengual, M. Khayet, M.P. Godino, Heat and mass transfer in vacuum membrane distillation, Int. J. Heat Mass Transfer, 47 (2004) 865–875.